Markovian Models of Solar Power Supply for a LTE Macro BS

Giuseppe Leonardi[1], Michela Meo[1], Marco Ajmone Marsan[1,2]
1 - Department of Electronics and Telecommunications - Politecnico di Torino, Italy
2 - IMDEA Networks Institute, Leganes (Madrid), Spain

***Abstract*—We consider a solar power supply for a LTE macro base station (BS) based on a photovoltaic (PV) panel and a battery, and we develop two discrete-time Markov chain (DTMC) models for the analysis and the dimensioning of the system elements (PV panel size and battery capacity). The DTMC models account for the solar irradiance levels in pairs or triples of consecutive days, and for the quantity of energy stored in the battery. From the DTMC steady-state (or transient) solution it is possible to derive performance metrics on which the system dimensioning can be based. We apply our models to BS locations in southern and northern Italy. Results show that the simpler model contains sufficient details for an effective system design.**

I. Introduction

The use of Renewable Energy Sources (RESs) to power Base Stations (BSs) of Radio Access Networks (RANs) is gaining increasing attention for a number of reasons. First, RANs, and the wide gamut of services they provide, are reaching countries where the power grid is either not available in large areas or unreliable for long periods of time. This means that BSs must be equipped with an autonomous power source, which can exploit either RESs or a Diesel power generator. The latter option is often much more expensive, specially for remote locations, when fuel transport (and possibly also fuel theft) becomes an issue. Second, the process of densification of RANs in urban areas implies the activation of large numbers of small cells, whose BSs must obviously be powered. Often, the connection of these BSs to the power grid is impractical, because of the administrative difficulties inherent in pulling cables across private and public properties. This makes the RES choice extremely attractive in small cell environments. Third, RESs seem to be the only viable option for the reduction of the energy costs of Mobile Network Operators (MNOs), since, after a decade of intense research in energy-efficient networking, not much has happened, except for the introduction of more energy-parsimonious equipment, so that energy costs keep going up. The RES option might be the way to bring those costs down, even in a period of very strong traffic growth [1].

Research in the field of RES-powered BSs and RANs started some years ago. The authors of [2], [3] provide a survey of recent publications in the field. In our previous works [4], [5] we tackled the design of the photovoltaic (PV) panel size and of the number of batteries to power a BS in different geographical locations, using the (deterministic) metereological data of the typical metereological year. In this paper we look at a probabilistic metereological model that we construct from public data of solar irradiation in the last twenty years, separately considering seasonal behaviors, in order to show that winter data should be considered in the system dimensioning. We actually consider two different Markovian models, one based on solar irradiation data in pairs of consecutive days, the other based on solar irradiation in triples of consecutive days, with the objective of verifying whether the correlation in the solar irradiation of consecutive days plays a significant role in the BS RES power performance. Results show that the two models are almost equivalent, so that the simpler one can be preferred. Markovian models similar to the ones presented here are proposed in [6], [7] for the computation of the BS outage probability. In [6] the model includes the hourly production in a day, while [7] distinguishes between weekend and working days that correspond to different levels of load on the BS.

II. Metereological Models

The procedure for dimensioning solar powered BSs equipped with a PV panel and a set of batteries starts with the stochastic characterization of solar radiation in the considered location.

For the characterization, we used the solar irradiance data available in SoDa [8], and in particular the NASA SSE and HelioClim databases, which provide the time series of daily solar radiation from July 1st 1983 to June 30th 2005. We take the daily mean irradiance, measured in $\mathrm{W\,m^{-2}}$, in the horizontal plane over 20 years, from 1985 to 2004. The daily irradiance values are then quantized on an integer number Q of levels: hence, each value of daily mean irradiance corresponds to an element of the set L of irradiance levels, with $L = \{L_1, L_2, ..., L_Q\}$.

From these data, we construct two discrete-time Markov chain (DTMC) models that differ in the degree of correlation among the irradiance of consecutive days. In the first model, called **1-day memory** model, the irradiance level in a day depends only on the irradiance in the previous day. In the **2-days memory** model, the irradiance level depends on the irradiance of two consecutive previous days.

The state of the 1-day memory DTMC is the level of daily mean irradiance in a single day, hence the state space cardinality is Q. The DTMC transition probabilities p_{ij} can be computed from traces collecting daily irradiance values in a given location. Let the sequence $\mathcal{I}$ represent the sequence of irradiance values; considering pairs of consecutive values, the probability p_{ij} is given by the relative frequence of

occurrence of the pair (L_i, L_j) over all pairs $(L_i, \cdot)$. The matrix $P^{(1)} = \{p_{ij}\}$ is the transition probability matrix of the DTMC.

The state of the 2-days memory model describes the levels of daily mean irradiance in two consecutive days, hence the number of states is Q^2. The transition probabilities p_{ijk} are the probabilities of moving from state (i, j) to state (j, k), with $i, j, k \in [1, Q]$. In order to compute the elements p_{ijk}, we look at triples of consecutive irradiance levels in the sequence $\mathcal{I}$, and count the recurrence of each possible triple (L_i, L_j, L_k). Note that from any state (i, j) it is possible to reach only states (j, k), and, hence, the transition probability matrix $P^{(2)}$ is a $Q^2 \times Q^2$ matrix where at most Q^3 non-zero elements exist.

III. Harvested and Consumed Energy Estimation

The BS daily energy consumption C depends on the traffic profile, and on the BS technology. We consider four alterntive types of traffic profile, referring to measures performed on an operational cellular network in business/residential areas, during weekdays and weekends [4]. As regards technology, we look at LTE BSs that either adopt a RRU (Remote Radio Unit) layout or not. The values reported in Table I are the resulting daily energy consumptions. In the following, for the sake of brevity, we will show results only for the weekend residential data, since they correspond to the highest energy demand.

TABLE I
Energy consumption of LTE BSs for different configurations. The values are in kWh.

	Residential Profile		**Business Profile**	
	with RRU	**w/o RRU**	**with RRU**	**w/o RRU**
Week day	15.5	23.8	15.2	23.9
Weed end	15.7	24.7	12.6	19.5

The energy harvested by the PV panel can be computed with the online tool PVWatts® Calculator [9], which allows several parameters to be set. We selected the *Premium* Module Type, and the *Commercial* System Type. All other parameters were left to their default values. With a *Premium* Module, the approximate efficiency is about 20%.

The tool returns, for each month, the harvested energy (in kWh), and to obtain the mean daily produced energy P_{d}, with a level of irradiance L_i, we proceed as follows. Let I_i be the mean value of daily irradiance computed among all available irradiance values belonging to the same level i; let I_{d} be the mean daily irradiance computed among all available irradiance values independently of what irradiance level they belong to. The energy P_i produced in a day with an irradiance level i is therefore:

$$P_i = \frac{P_{\mathrm{d}}}{I_{\mathrm{d}}} I_i. \tag{1}$$

IV. Base Stations Models

To evaluate the performance of the BS power system, we develop a DTMC model which accounts for the battery charge level. We thus combine one of the previously described meteorological models with the description of the battery charge level.

We start by considering the 1-day memory meteorological model. The DTMC state is defined by the irradiance level in a day and by the battery charge level when the considered day begins.

Battery charge level x corresponds to an amount of energy stored in the battery equal to xB/N, where B is the total battery capacity in kWh, and $N + 1$ is the number of battery charge levels. The DTMC state is

$$(i, x) \quad \text{with} \begin{cases} i = 1, \cdots, Q \\ x = 0, \cdots, N \end{cases}$$

The amount of energy in the battery at the end of a day depends on the energy harvested by the PV panel (which in turn depends on the mean daily irradiance level and on the dimension of the PV panel) and on the BS energy consumption C (which depends on the traffic and on the power model of the BS) during the same day. For simplicity, we assume that C is constant.

In the DTMC, state (j, x) is reachable from states (i, y) with $yB/N = xB/N - \Delta E_i$ and $\Delta E_i = P_i - C$; P_i is the harvested energy in a day with irradiance level L_i and C is the daily energy consumption. The transition from state (i, y) to (j, x) occurrs with probability p_{ij}.

For the 2-days memory meteorological model, that accounts for triples of consecutive days, the DTMC state definition comprises three components (j, k, x): j is the irradiance level of the previous day, k the irradiance level of the current day, and x the battery charge level when the current day begins. State (j, k, x) is reachable from states (i, j, y), where $yB/N = xB/N - \Delta E_j$ and $\Delta E_j = P_j - C$, with probability p_{ijk}.

Note that we assume an idealized battery behavior, where all the energy stored in the battery can be retrieved from it, and the battery discharge does not depend on the starting level. Losses in efficiency in the battery behaviour can be compensated by slight overdimensioning of the PV panel.

A. Performance indicators

We evaluate the performance of the BS powering system from the steady-state probabilities. In the following, we report the performance indicators computed from the 1-day and 2-days memory models, denoting with $\pi^{(1)}_{i,y}$ and $\pi^{(2)}_{i,j,y}$ the steady-state probability that the two DTMCs are in states (i, y) and (i, j, y), respectively.

Outage probability: The outage probability, or discharged battery probability, is given by the probability that the battery charge is 0,

$$P(0)^{(1)} = \sum_{i=1}^{Q} \pi^{(1)}_{i,0}, \qquad P(0)^{(2)} = \sum_{i=1}^{Q} \sum_{j=1}^{Q} \pi^{(2)}_{i,j,0}. \tag{2}$$

Fully charged battery probability: The fully charged battery probability is the probability that the battery charge is equal to 100%,

$$P(100)^{(1)} = \sum_{i=1}^{Q} \pi_{i,N}^{(1)}, \qquad P(100)^{(2)} = \sum_{i=1}^{Q}\sum_{j=1}^{Q} \pi_{i,j,N}^{(2)}. \quad (3)$$

Wasted energy: The wasted energy, measured in kWh, is given by the weighted sum of the amount of energy that cannot be stored in the battery, because more energy is produced than what is needed, and the extra-produced energy is too much to be stored in the battery,

$$\begin{aligned} W^{(1)} &= \sum_{i=1}^{Q} \sum_{y \in S_j} (yB/N + \Delta E_j - B)\ \pi_{i,y}^{(1)} \\ W^{(2)} &= \sum_{i=1}^{Q}\sum_{j=1}^{Q} \sum_{y \in S_j} (yB/N + \Delta E_j - B)\ \pi_{i,j,y}^{(2)} \quad (4) \end{aligned}$$

where S_j is the set of values of battery charge such that some harvested energy is wasted because it cannot be stored in the battery,

$$S_j = \{y | yB/N + \Delta E_j > B\} \quad (5)$$

Virtual energy: The virtual energy, measured in kWh, represents the amount of energy that the BS needs, but cannot be provided by the RES powering system. In case of a BS powering system with back-up power supply, the virtual energy can be obtained from the backup system; otherwise, the BS must be powered off,

$$\begin{aligned} V^{(1)} &= \sum_{i=1}^{Q} \sum_{y \in T_j} (-yB/N - \Delta E_j)\ \pi_{i,y}^{(1)} \\ V^{(2)} &= \sum_{i=1}^{Q}\sum_{j=1}^{Q} \sum_{y \in T_j} (-yB/N - \Delta E_j)\ \pi_{i,j,y}^{(2)} \quad (6) \end{aligned}$$

where T_j is the set of values of battery charge such that the sum of the stored energy and the harvested energy is not enough to satisfy the BS energy need,

$$T_j = \{y | yB/N + \Delta E_j < 0\} \quad (7)$$

Average harvested energy: Finally, the average harvested energy is given by

$$P_h^{(1)} = \sum_{i=1}^{Q}\sum_{y=0}^{N} P_j\ \pi_{i,y}^{(1)}. \qquad P_h^{(2)} = \sum_{i=1}^{Q}\sum_{j=1}^{Q}\sum_{y=0}^{N} P_j\ \pi_{i,j,y}^{(2)}. \quad (8)$$

V. Numerical Results - Catania

We start by considering the city of Catania in Italy, during meteorological winter, choosing $Q = 5$ quantization levels for the daily irradiance values. Moreover, we discuss the differences in results between the 1-day and 2-days memory models, as well as the differences between the summer and winter cases.

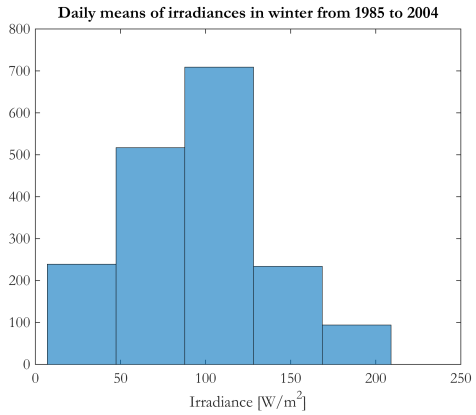

Fig. 1. Daily mean irradiance distribution for Catania in winter.

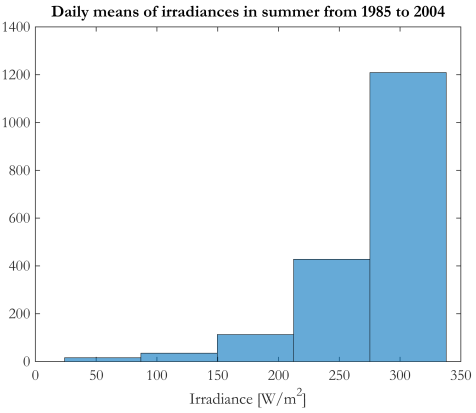

Fig. 2. Daily mean irradiance distribution for Catania in summer.

Most result curves are plotted versus the PV system size [9], which is the DC power rating of the photovoltaic array in kilowatts (kW) at standard test conditions (STC - solar irradiance of 1 kW/m^2, cell temperature of 25 °C and air mass of 1.5).

The histograms of the mean daily irradiance in Catania, using a quantization on 5 levels, can be seen in Figures 1 and 2 for the winter months (December, January, February) and for the summer months (June, July, August). As expected, differences are large (a factor between 2 and 3 applies to the overall monthly averages, see Table II, because of both longer hours of daylight and better weather), and winter is the season with the lowest values of daily irradiance, hence critical for the dimensioning of the BS. For this reason, we focus our attention on the solar radiation data of December, January and February from 1985 to 2004.

TABLE II
Monthly harvested energy in winter and summer computed using PVWatts® in Catania.

	Dec	Jan	Feb	Jun	Jul	Aug
Energy [kWh]	248	255	355	660	718	667

From the monthly average energy in December, January and

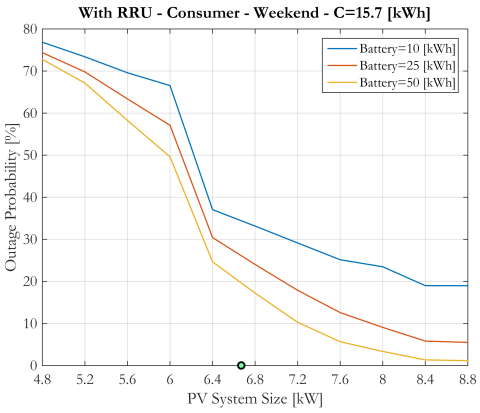

Fig. 3. Outage probability vs PV panel's size for several battery capacities when $\boldsymbol{C = 15.7}$ kWh. The marker on the $\boldsymbol{x}$-axis represents the point at which the chain is balanced, i.e., the average produced energy is equal to the consumed energy.

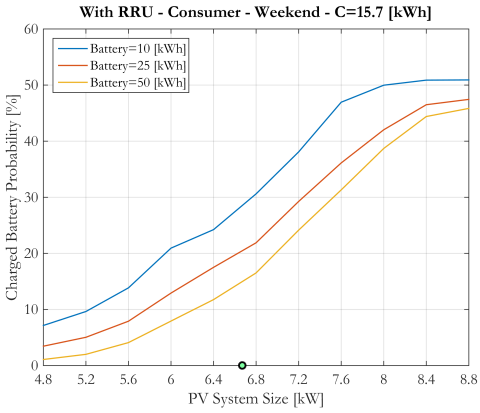

Fig. 4. Charged battery probability vs PV panel's size for several battery capacities when $\boldsymbol{C = 15.7}$ kWh.

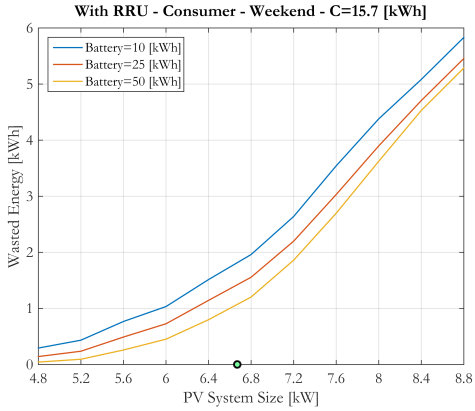

Fig. 5. Wasted energy vs PV panel's size for several battery capacities when $\boldsymbol{C = 15.7}$ [kWh].

February, the daily harvested energy in meteorological winter can be easily computed.

Considering a LTE BS with a "residential" traffic profile, adopting the remote radio unit (RRU) layout, and assuming to be in weekend days, the average energy consumption is equal to $C = 15.7$ kWh (see Table I).

In Figure 3 we show the results produced by the 2-days memory model for the BS outage probability, for three different values of battery capacity, versus the PV panel size. As expected, fixing the value of the battery capacity, the probability that the battery discharges decreases as the panel size increases. Fixing the size of the PV panel, the outage probability becomes lower as the battery capacity increases. If the power system design aims at an outage probability of the order of 1%, the curves tell us that a PV system power of the order of 8.5 kW and a battery of capacity 50 kWh are necessary.

The steep transition in the discharged battery probability, observable when the PV System size is around 6.2 kW, is due to quantization effects. The jump occurs when the vector of the values of ΔE_i comprises at least one element which, from a negative value, assumes a positive value or zero. The curve becomes smoother when the number Q of quantization levels of irradiance is increased, as we will show in section V-B.

Figure 4 shows the fully charged battery probability in the same conditions. For each battery capacity value, the probability that the battery is fully charged increases as the PV panel's dimension increases. For a given PV panel's size, the higher the battery capacity, the lower the charged battery probability.

Figure 5 shows the amount of energy produced by the PV panel that cannot be stored in the battery because it is already fully charged. Clearly, the amount of wasted energy increases as the PV panels size increases and decreases as the battery capacity increases. With a dimensioning of the power system that gives an outage probability of the order of 1% (PV panel of 8.5 kW and battery of 50 kWh), almost 5 kWh per day are lost on average.

Figure 6 shows the amount of energy which should be consumed by the BS, but is not available in the battery, because it is already fully depleted. This amount of energy becomes lower as the energy production and the battery capacity increase, and it is very small for the system parameters yielding a 1% outage probability.

Figure 7 shows all contributions, allowing the reader to verify the energy balance: all the energy that enters the battery has to be extracted from the battery itself. Therefore the plotted quantities are:

- P_h, average amount of energy harvested by the PV panel
- C, daily energy consumption (assumed to be constant)
- W, that part of P_h which does not enter the battery, because the battery is already fully charged (wasted energy)
- V, that part of C which cannot be consumed, being the battery discharged (virtual energy).

Hence, the actual energy which enters the battery is

$$P' = P_h - W \tag{9}$$

and the actual consumption is

$$C' = C - V. \tag{10}$$

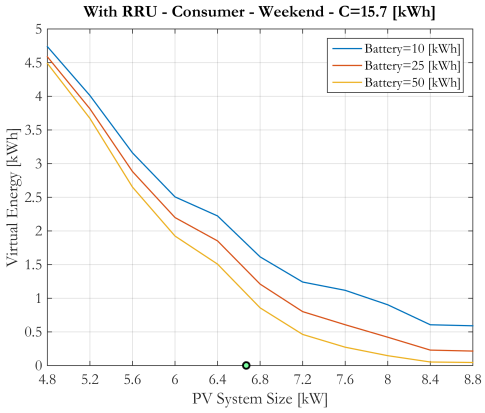

Fig. 6. Virtual energy vs PV panel's size for several battery capacities when $\boldsymbol{C = 15.7}$ [kWh].

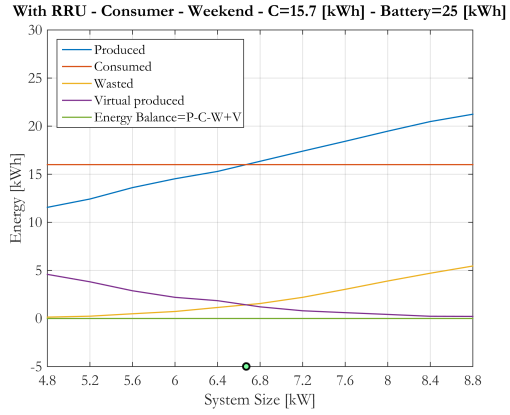

Fig. 7. Energy balance vs PV panel's size when the battery capacity is $\mathbf{25}$ kWh.

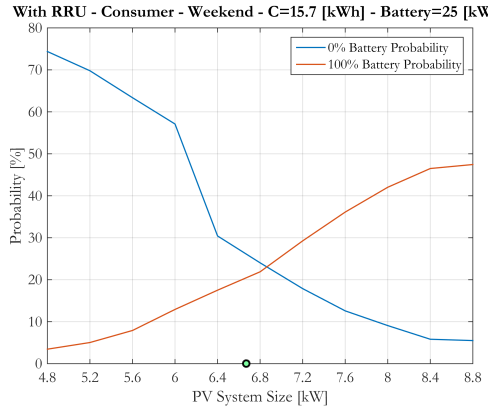

Fig. 8. Discharged and charged battery probabilities vs PV panel's size when the battery capacity is $\mathbf{25}$ kWh.

Clearly, the following relation must be satisfied:

$$P' - C' = P_h - W - C + V = 0. \tag{11}$$

Results equivalent to Figure 3, assuming the LTE BS does not adopt a RRU configuration (so that $C = 24.7$ kWh - see Table I) are plotted in Figure 9.

Figure 10 shows, for the same BS configuration, the discharged and charged battery probabilities versus the battery

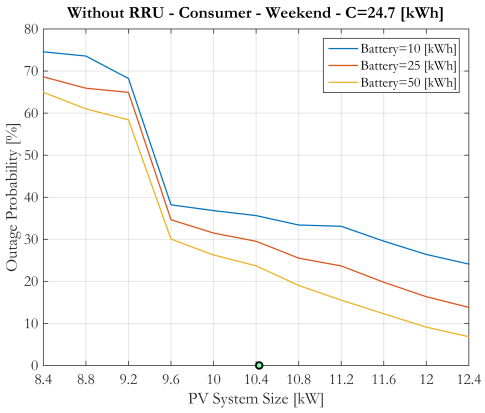

Fig. 9. Outage probability vs PV panel's size for several battery capacities when $\boldsymbol{C = 24.7}$ kWh.

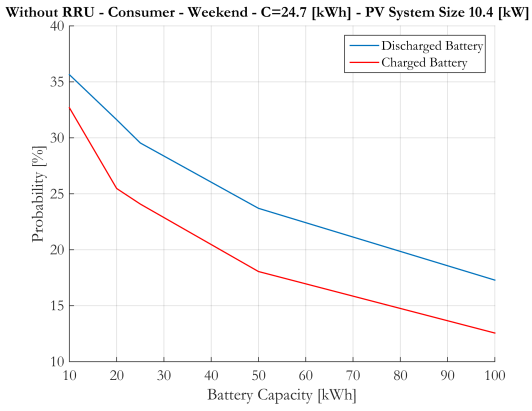

Fig. 10. Discharged and charged battery probability vs battery capacity when $\boldsymbol{C = 24.7}$ kWh and the PV panel's size is $\mathbf{10.4}$ kW.

capacity, with PV system size set to 10.4 kW. This value is very close to the equilibrium point, indeed the probabilities are similar.

Finally, we compare the results obtained using the 1-day memory and 2-days memory models of solar irradiance. We assume a daily energy consumption equal to $C = 24.7$ kWh and a battery capacity $B = 25$ kWh. Note that the results shown so far used the model based on 2-days memory. Figure 11 and Figure 12 report, respectively, the discharged and the charged battery probability computed by the two models: on average, both probabilities are slightly higher for the more detailed model, but results are quite similar. The same can be said for the wasted and the virtual energies (not reported for brevity). In general, relative differences remain below 10% for PV system sizes whose production roughly balances the daily energy consumption. This means that the gain achieved with the more refined model is small.

A. *Winter vs Summer*

While it is clear that winter, having the lowest value of average solar irradiation, is the most relevant period for dimensioning a solar power system for the LTE BS, it can be interesting to discuss what happens in more favorable

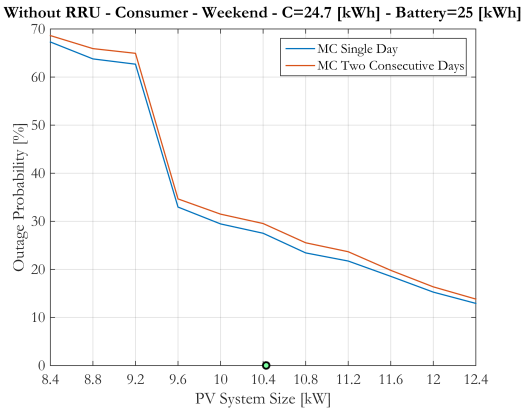

Fig. 11. Outage probability vs PV panel's size for both employed metereological models when $\boldsymbol{C = 24.7}$ kWh and the battery capacity is $\boldsymbol{B = 25}$ kWh.

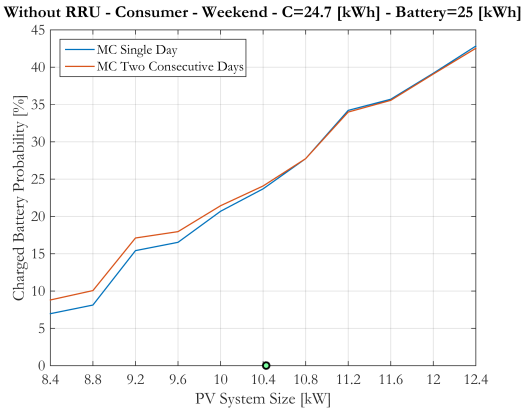

Fig. 12. Charged battery probability vs PV panel's size for both employed metereological models when $\boldsymbol{C = 24.7}$ kWh and the battery capacity is $\boldsymbol{B = 25}$ kWh.

periods of the year. For this reason, we plot in Figure 13 the BS outage probability due to energy depletion. As expected, this probability is almost zero at the same PV System sizes exploited in winter. Again as expected, the waste of energy is huge (see Figure 14). This means that dimensioning the BS power system for the winter period implies a large energy surplus in summer, but also that dimensioning over the yearly average implies an energy transfer from summer to winter, which may be problematic and costly in terms of the necessary battery capacity. Of course, dimensioning for the summer period yields unacceptable performance in winter.

B. Number of irradiance levels

The choice of the number Q of irradiance levels partially modifies the output of the models. Indeed, increasing the number of irradiance levels produces smoother transitions with respect to the previous plots, but the computational time required to solve the DTMC models increases. Figures 15 and 16 show the outage and charged battery probabilities for several values of Q. Note that the choices $Q = 8, 10$ allows smoothing the jump observed in the outage probability with $Q = 5$ (Figure 3).

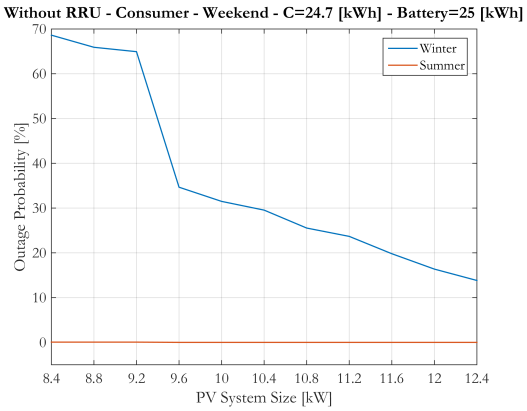

Fig. 13. Outage probability vs PV panel's size in winter and summer when $\boldsymbol{C = 24.7}$ kWh and the battery capacity is $\boldsymbol{B = 25}$ kWh.

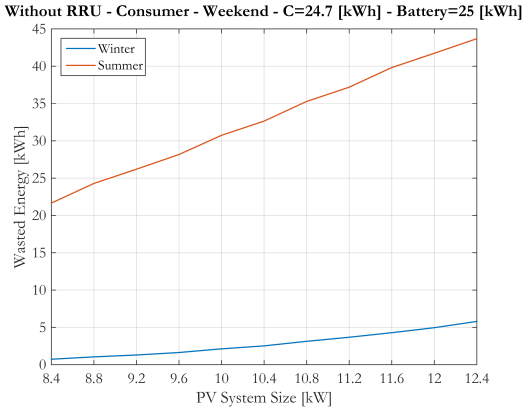

Fig. 14. Wasted energy vs PV panel's size in winter and summer when $\boldsymbol{C = 24.7}$ kWh and the battery capacity is $\boldsymbol{B = 25}$ kWh.

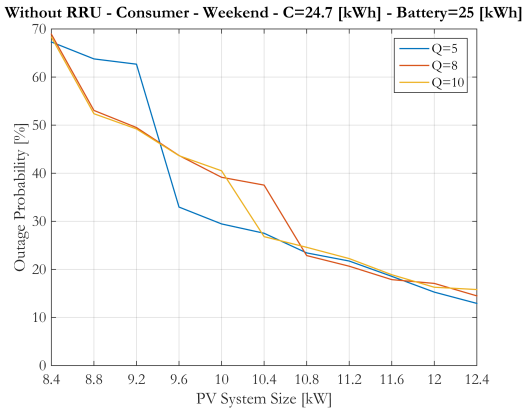

Fig. 15. Outage probability vs PV panel's size for different quantization levels of irradiance when $\boldsymbol{C = 24.7}$ kWh and the battery capacity is $\boldsymbol{B = 25}$ kWh.

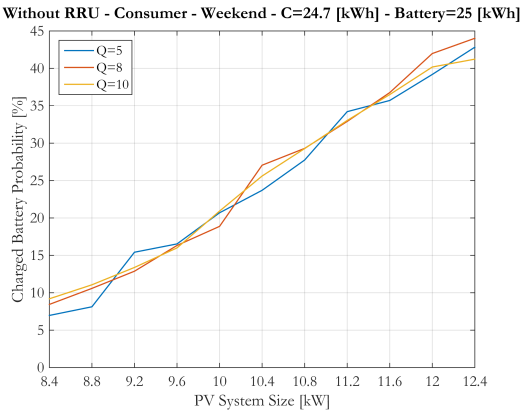

Fig. 16. Charged battery probability vs PV panel's size for different quantization levels of irradiance; $\boldsymbol{C = 24.7}$ kWh and $\boldsymbol{B = 25}$ kWh.

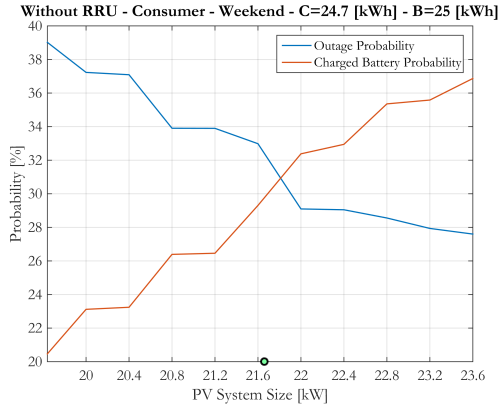

Fig. 17. Discharged and charged battery probabilities vs PV panel size; $\boldsymbol{C = 24.7}$ kWh and $\boldsymbol{B = 25}$ kWh.

VI. The Torino Location

To evaluate how much the geographical location impacts the characterization of the energy flows in a RES base station, we now look at the case of Torino, considering solar radiation data of December, January and February from 1985 to 2004 (as done for Catania). As expected, on average the amount of solar radiation in northern Italy is less than the one in Catania. The monthly harvested energies from a PV panel at the same conditions of Table II are shown in Table III.

TABLE III
Monthly harvested energy in meteorological winter computed using PVWatts® in Torino.

	Dec	Jan	Feb
Energy [kWh]	110	122	179

Figure 17 reports the discharged and charged battery probabilities versus the PV system size. The equilibrium point, assuming the battery capacity equal to $B = 25$ kWh, is approximately 21.7 kW, roughly double the value of the case of Catania. Figure 18 shows the energy balance and the wasted and virtual energies as the PV system size varies.

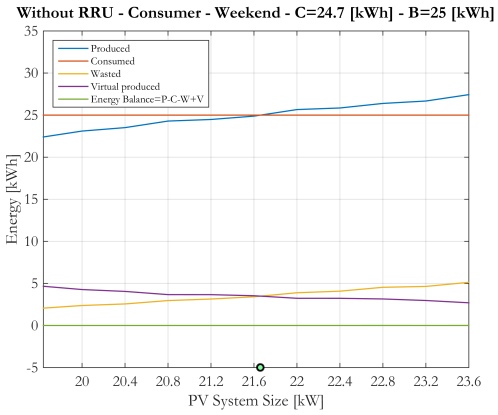

Fig. 18. Energy balance vs PV panel size; $\boldsymbol{C = 24.7}$ kWh and $\boldsymbol{B = 25}$ kWh.

VII. Conclusion

We described two DTMC models that can be used for dimensioning the solar power supply of a LTE macro BS. The DTMC models account for the solar irradiance levels in pairs or triples of consecutive days, and for the quantity of energy stored in the battery. By applying our models to BS locations in southern and northern Italy we observed that the resulting system dimensioning is not significantly influenced by the longer memory. We also observed that the number of quantization levels for both irradiance and battery charge must be carefully chosen, and that seasonal behaviors are (obviously) of key importance in the dimensioning.

Acknowledgement

M. Ajmone Marsan was supported in part by the European Union through the Xhaul project (H2020-ICT-671598) and in part by Ministerio de Economía y Competitividad grant TEC2014-55713-R. The statements made herein are solely the responsibility of the authors.

References

[1] Cisco, "Cisco Visual Networking Index: Global Mobile Data Traffic Forecast Update, 2013-2018," http://www.cisco.com/.
[2] H. Hassan, L. Nuaymi, A. Pelov, "Renewable Energy in Cellular Networks: a Survey," *IEEE OnlineGreenComm*, October 2013.
[3] A. M. Aris, B. Shabani, "Sustainable Power Supply Solutions for Off-Grid Base Stations," Energies 2015, 8, 10904-10941; doi:10.3390/en81010904
[4] M. Ajmone Marsan, G. Bucalo, A. Caro, M. Meo, Y. Zhang, "Towards Zero Grid Electricity Networking: Powering BSs with Renewable Energy Sources", *IEEE ICC'13*, pp.596-601, 9-13 June 2013
[5] M. Meo, Yi Zhang, R. Gerboni, M. Ajmone Marsan, "Dimensioning the power supply of a LTE macro BS connected to a PV panel and the power grid," *IEEE International Conference on Communications (ICC),* pp. 178 - 184, 8-12 June 2015.
[6] V. Chamola and B. Sikdar, "Resource Provisioning and Dimensioning for Solar Powered Cellular Base Stations", *IEEE GLOBECOM,* Austin, USA, Dec. 2014
[7] Vinay Chamola, Biplab Sikdar, "Outage Estimation for Solar Powered Cellular Base Stations," *IEEE International Conference on Communications (ICC),* pp. 172 - 177, 8-12 June 2015.
[8] SODA, http://www.soda-is.com/eng/index.html.
[9] PVWatts, http://rredc.nrel.gov/solar/calculators/pvwatts/version1/.